Transactions of the Indian National Academy of Engineering (2021) 6:839–855
https://doi.org/10.1007/s41403-021-00251-w

ORIGINAL ARTICLE

Tailoring the Microstructure and Mechanical Properties of Titanium Alloy Ti6Al4V Forgings with Different Combinations of Thermo-Mechanical Processing and Heat Treatment Cycles

Pravendra Pratap Singh[1] · **R. K. Gupta**[2] · **V. Anil Kumar**[2] · **Ravi C. Gundakaram**[3] · **Satish Kumar Singh**[2]

Received: 14 May 2021 / Accepted: 3 July 2021 / Published online: 13 July 2021

Abstract

Thermo-mechanical processing has been carried out on titanium alloy Ti6Al4V blocks at 50 °C intervals in the temperature range of (800–1000 °C) and with different amounts of reduction (25%, 50% and 75%). Further, mill annealing (MA) and recrystallization annealing (RA) heat treatment cycles were employed on the as-forged samples. With an increase in % reduction, the refinement in α phase has been observed in the samples forged below β transus temperature (T_{β}) resulting in higher tensile strength and reduction in impact strength in 'MA' condition. 25% reduction followed by 'RA' heat treatment and 50–75% reduction followed by 'MA' heat treatment resulted in marginally lower tensile strength, which is attributed to presence of higher volume fraction (V_f) of recrystallized α. Higher impact strength is observed in samples forged above or near T_{β} of the alloy and can be attributed to the presence of higher volume fraction (V_f) of transformed β. 50% reduction is found to be effective in achieving significant microstructural refinement of α and thereby higher strength in both MA and RA heat treated conditions.

Keywords Titanium alloy · Ti6Al4V · Forging · Mill annealing · Recrystallization annealing · Microstructure · Fractography

Introduction

Titanium alloy Ti6Al4V is widely used in aerospace, power generation, automotive, applications due to high specific strength and high corrosion resistance in aggressive environments and in biomedical applications due to its good biocompatibility (Chong et al. 2019; Shaikh et al. 2019; Prasad and Kumar 2011; Lin et al. 2018). The microstructure of the materials plays an important role in governing the mechanical properties such as ductility, tensile strength, fracture toughness and crack propagation resistance in the materials (Kim and Boyer 1991; Lütjering et al. 1994). The microstructure and resultant mechanical properties depend primarily on the chemical composition, history of thermomechanical processing and thermal treatment (Ding et al. 2002). Thermomechanical processing is a very useful method for refinement of the microstructure, e.g. controlling the size of the α, optimizing the ratio of the α and β phases, and controlling the morphology of α and β phases (Ding and Guo 2004; Chao et al. 2016). The Ti6Al4V alloy has been extensively studied by a large number of researchers. Previous studies have shown that thermomechanical processing of the $(\alpha+\beta)$ titanium alloy in the β-phase field leads to a lamellar microstructure after cooling to room temperature (Flower 1990; Lütjering 1998). Subsequent deformation in $(\alpha+\beta)$ phase field and heat treatment by varying cooling rate and heat treatment temperature can result in microstructure ranging from acicular to equiaxed. In addition to processing temperature, other hot working parameters such as strain also influence the microstructure, e.g. the V_f of α and β phases and the size of α (Gerhard et al. 1993; Nieh et al. 2005; Seshacharyulu et al. 2000).

✉ V. Anil Kumar
vesangiak@gmail.com

1 Department of Chemistry, Indian Institute of Space Science and Technology, Trivandrum 695547, India

2 Materials and Mechanical Entity, Vikram Sarabhai Space Centre, Trivandrum 695022, India

3 Centre for Materials Characterization and Testing, International Advanced Research Centre for Powder Metallurgy and New Materials, Hyderabad 500005, India

Thus, microstructure evolution during hot working is influenced by the initial microstructure, hot working temperature, strain, strain rate and subsequent cooling rate (Guo et al. 2005; Gupta et al. 2016; Welsch et al. 1988; Seetharaman et al. 1991; Gupta et al. 2018a, b; Smith 1993). The morphology of α phase can vary between equiaxed, plate-like, basket weave, Widmanstätten or acicular with different hot working temperatures and cooling rates (Shaikh et al. 2019; Flower 1990). Desired microstructure can be obtained by using suitable parameters. However, problems still persist at industrial scale in hot deformation to obtain defect-free forged/ rolled products of ultrasonic quality class A1 as per AMS 2631-2017 standard (1.2 mm flat bottom hole or equivalent size indications) for aerospace applications (Gupta et al. 2007). Such products are used to realize very thin section components, where defect tolerances are very low. To obtain such sound ultrasonic quality forgings, the deformation temperature is suggested to be in the vicinity of 900 °C, which is quite difficult to maintain especially for large-sized products (Gupta et al. 2018a, b). Also, obtaining uniform mechanical properties in large-sized products (with very less scatter) is another challenge faced by titanium alloy product mills. It is important to understand the mechanical properties of titanium alloy Ti6Al4V in various conditions, which assumes great significance to design a particular forging operation and/ or heat treatment cycle. It may be noted that a systematic study simulating industrial practice of forging followed by heat treatment and its effect on tensile as well as impact properties of the Ti6Al4V alloy has not been reported. Thus, to bring out a better understanding on the effect of deformation temperature and heat treatment on the microstructural evolution and mechanical properties of Ti6Al4V, the present study is carried out.

The objective of this study was to investigate the effect of different forging reduction percentages and different annealing processes on the microstructure and mechanical properties of Ti6Al4V simulating its industrial scale processing. The influence of hot working parameters such as strain and temperature on the changes in microstructure and changes in mechanical properties has been investigated in the present work.

The β transus temperature (T_{β}) of the Ti6Al4V alloy under study is 992 °C, which is similar to calculated value of ~ 995 °C (Guo et al. 2005). In order to achieve the above mentioned objectives, the forging has been done to different % reductions of 25, 50 and 75% at different temperatures varying from the lower ($\alpha+\beta$) phase field (i.e. 800 and 850 °C), intermediate ($\alpha+\beta$) phase field (e.g. 900 °C), higher ($\alpha+\beta$) phase field (i.e. 950 °C) and in the single-phase β field (i.e. 1000 °C). There are components in aerospace applications such as liners for composite over-wrapped pressure vessels and other hostile applications in power sector, chemical industry as well as biomaterials sector where uniform mechanical properties are desired. In such cases recrystallization annealing (RA) is more appropriate to achieve a uniform and refined microstructure (Gupta et al. 2016). Considering all these aspects, a systematic investigation has been conducted in the present work. Similar works mentioned above have been reported with lab-scale studies in isolation. However, a systematic approach of hot working with different % reduction and with different post work annealing on industrial scale is the prime focus of this work, which is not reported earlier.

Material and Methods

The chemical composition of the as-received (AR) material is Ti-6.2Al-4.2 V-0.19O-0.05Fe. The as-received material was in hot forged + annealed at 730 °C- 2 h-A/C to RT in the form of rectangular cross-section blocks of size $70 \times 70 \times 100$ mm^3. The blocks were preheated in an electric furnace for 2 h at different temperatures (i.e. 800 °C, 850 °C, 900 °C, 950 °C and 1000 °C). Preheating temperature was set to 10 °C higher than the deformation temperature for duration of 10 min just before taking out the job from the furnace so as to compensate for the estimated heat loss due to handling during forging. The blocks were upset hot forged along the highest dimension direction (100 mm) using a hydraulic forging press of 1000 MT capacity to different percentage reductions (i.e. 25%, 50%, 75%). The forging operations were carried out without any reheating. Strain rate during deformation was ~ 0.1 s^{-1}.

After the forging operation, the blocks were air cooled to room temperature. Subsequently, forged blocks were cut into two halves. One half was taken for mill annealing (MA) at 730 °C for 2 h in a muffle furnace followed by furnace cooling to room temperature. The second half was taken for recrystallization annealing (RA) at 930 °C for 1 h in the same muffle furnace followed by furnace cooling to room temperature. After completion of both types of annealing heat treatments, the microstructure evaluation and mechanical testing were carried out. Additionally, another set of samples in as-received (AR) condition was heat treated at different temperatures (e.g. 800, 850, 900, 950 and 1000 °C) for 1-h duration followed by air cooling to room temperature to compare the effect of heat treatment alone with that of coupons subjected to forging at these temperatures followed by RA and MA heat treatments. The identification details of samples denoted in the manuscript are given in Table 1. Subsequently, 'M' for mill annealing and 'R' for recrystallization annealing have been put as suffixes in sample designation. Grain size and volume fraction (V_f) referred throughout the paper are for the α phase. The alloy samples were characterized for microstructure in different conditions viz. as-received (AR), AR + heat treated (HT), as-forged + heat

Table 1 Identification of heat-treated and forged samples of Ti6Al4V used in present study

Heat treatment/forging start temperature, (°C)	Heat treated samples	Hot forged with (%) reduction-AF			Hot forged + Mill annealed (MA)- 'M'/Recrystallization annealed (RA)-'R'		
		25%	50%	75%	25%	50%	75%
1000	A	A2	A5	A7	A2M/R	A5M/R	A7M/R
950	B	B2	B5	B7	B2M/R	B5M/R	B7M/R
900	C	C2	C5	C7	C2M/R	C5M/R	C7M/R
850	D	D2	D5	D7	D2M/R	D5M/R	D7M/R
800	E	E2	E5	E7	E2M/R	E5M/R	E7M/R

treated (AF + MA and AF + RA). Microstructural observations have been carried out using Olympus-make GX71 optical microscope (OM) and fractography analysis of tensile-tested and impact-tested samples was carried out using Carl Zeiss Sigma HD Field Emission Scanning Electron Microscope (FESEM).

The samples for electron back scattered diffraction (EBSD) analysis were prepared by conventional metallographic polishing followed by fine colloidal silica polishing. The samples were then subjected to electro polishing using 80% methanol, 20% perchloric acid mixture at a temperature of − 25 °C, voltage of 11 V for 30 s in Struers-make Lectropol-5 model electro polishing machine. EBSD measurements were performed in a Carl Zeiss field emission scanning electron microscope, model Gemini 500. The EBSD maps were recorded on a scan area of 300 µm × 200 µm and step size of 0.3 µm. For further analysis step size of 0.05 µm was also used for selected samples. The EBSD data were analyzed using TSL OIM software, version 8.

Tensile testing was carried out using Zwick Roell universal testing machine (UTM) and impact strength was evaluated using INSTRON-make impact testing machine. All the test samples were taken from the core of the forging and along the direction perpendicular to forging axis. Three tensile and three impact test specimens representative of each condition were tested. The size of α and its V_f was estimated from the optical microstructures using ImageJ™ software as well as through EBSD. The input material, forging process and blocks subjected to different reductions imparted on blocks are shown in Fig. 1.

Results and Discussion

Microstructure Analysis

The microstructure of the as-received (AR) Ti6Al4V alloy presented in Fig. 2a consists of equiaxed α phase in transformed β matrix. The phases were uniformly distributed in the microstructure (bright phase indicates α grains and dark phase indicates transformed β phase). The average grain size and V_f of equiaxed α phase was 26 ± 3 µm and 42 ± 5%, respectively.

Effect of Heat Treatment

The samples which had undergone heat treatment below T_β showed that both phases (α and β) were uniformly distributed. The grain size distribution of α was almost of same with ± 3 µm variation for the heat treatment conditions up to 900 °C. The V_f of α was also within ± 5% variation for the heat treatment conditions up to 900 °C. The representative

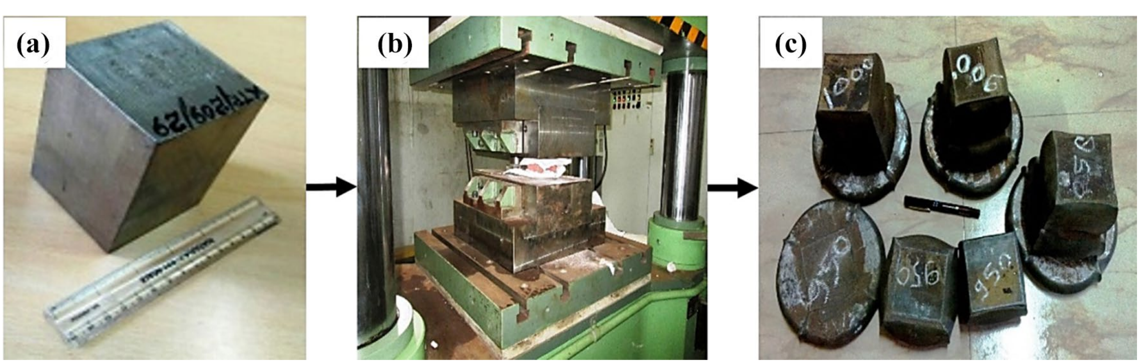

Fig. 1 Photographs showing **a** as-received Ti6Al4V material, **b** forging in a hydraulic press and **c** as-forged Ti6Al4V blocks forged to different % reduction

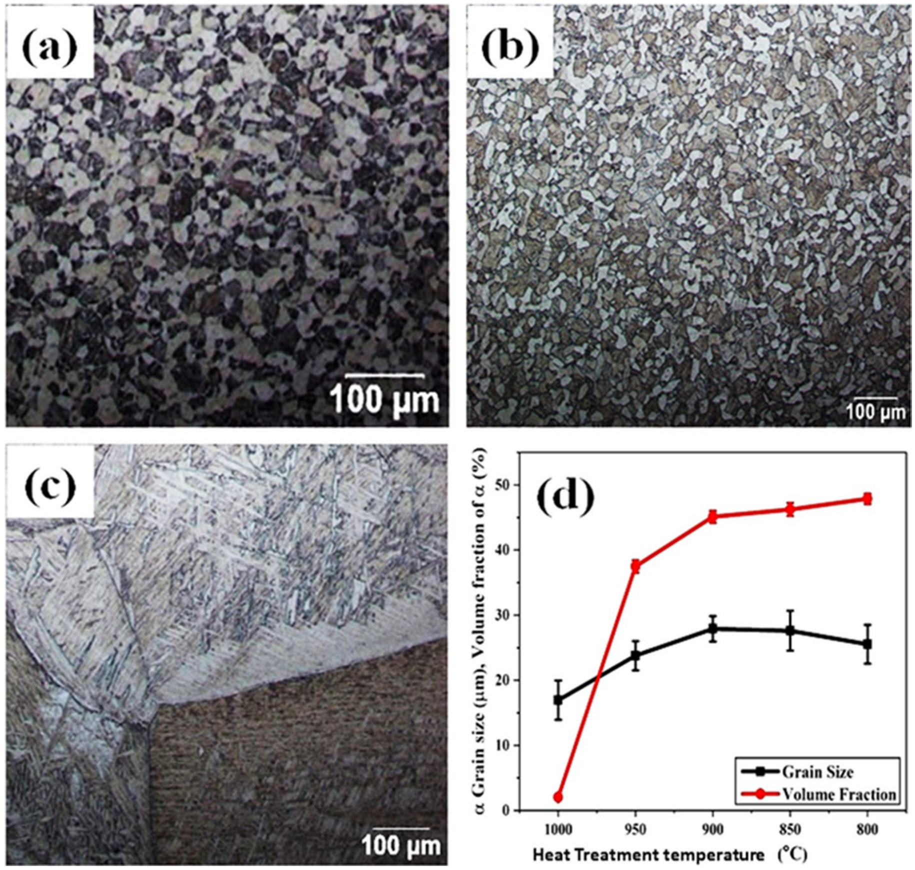

Fig. 2 OM Images of Ti6Al4V forgings **a** representing as-received (AR) sample in mill-annealed condition, **b** heat treated at 950 °C, **c** heat treated at 1000 °C and **d** variation in α grain size and V_f of α with heat treatment temperature

photomicrograph of 'AR' sample in forged and milled annealed condition is presented in Fig. 2a. The microstructure of the sample heat treated at 950 °C (near T_β) as shown in Fig. 2b shows lower amount of α. In the samples which had undergone soaking at temperature above T_β (1000 °C), the microstructure was found to be of Widmanstätten structure with isolated acicular α phase (Fig. 2c) and almost no primary alpha. The variation in α grain size (section of acicular grain) and V_f of α phase with heat treatment temperature is shown in Fig. 2d. Acicular α grains were found to have aspect ratios in the range of 5–6. The α grain size and V_f both were found to decrease with increase in heat treatment temperature near to the T_β of the alloy.

Effect of % Reduction and Heat Treatment

The as-forged samples were subjected to mill annealing and recrystallization annealing heat treatment cycles and analyzed for microstructure as shown in Figs. 3, 4 in all the three forged conditions (25%, 50%, 75% reduction). Mill annealing is not expected to alter the microstructure of as-forged (AF) condition samples significantly, but for reducing the residual stresses, since it is well below the T_β (~ 995 °C). Only minor changes are expected in V_f of α according to % reduction imparted along with different reduction temperature. Whereas recrystallization heat treatment is carried out ~ 50 °C below the T_β, which can alter the microstructure significantly. The same is observed in the present work as well.

Effect of Combination of Forging and Mill Annealing Heat Treatment

In the case of 25% reduction samples subjected to mill annealing, it is observed that when forging was carried out below T_β, the α grain size (Fig. 3a) was 30 ± 3 µm and V_f of α phase was 40 ± 2% with respect to different forging temperatures. In case of sample forged above T_β followed by MA (Fig. 3b, c), larger transformed β grains containing α acicular/ Widmansttaten type of laths of finer alpha within them with lower V_f of α are observed. However, when finish forging temperature is below T_β, although the start temperature is above T_β, the β grain size is reduced and equiaxed α evolves. In the sample shown in Fig. 3b, c, the V_f of α phase was also higher as compared to sample subjected to heat treatment alone at the corresponding temperature. Microstructure was Widmanstätten laths of α in transformed β matrix with very little amount of α phase in Fig. 3b, c which is due to finish temperature being below T_β during which α phase evolves.

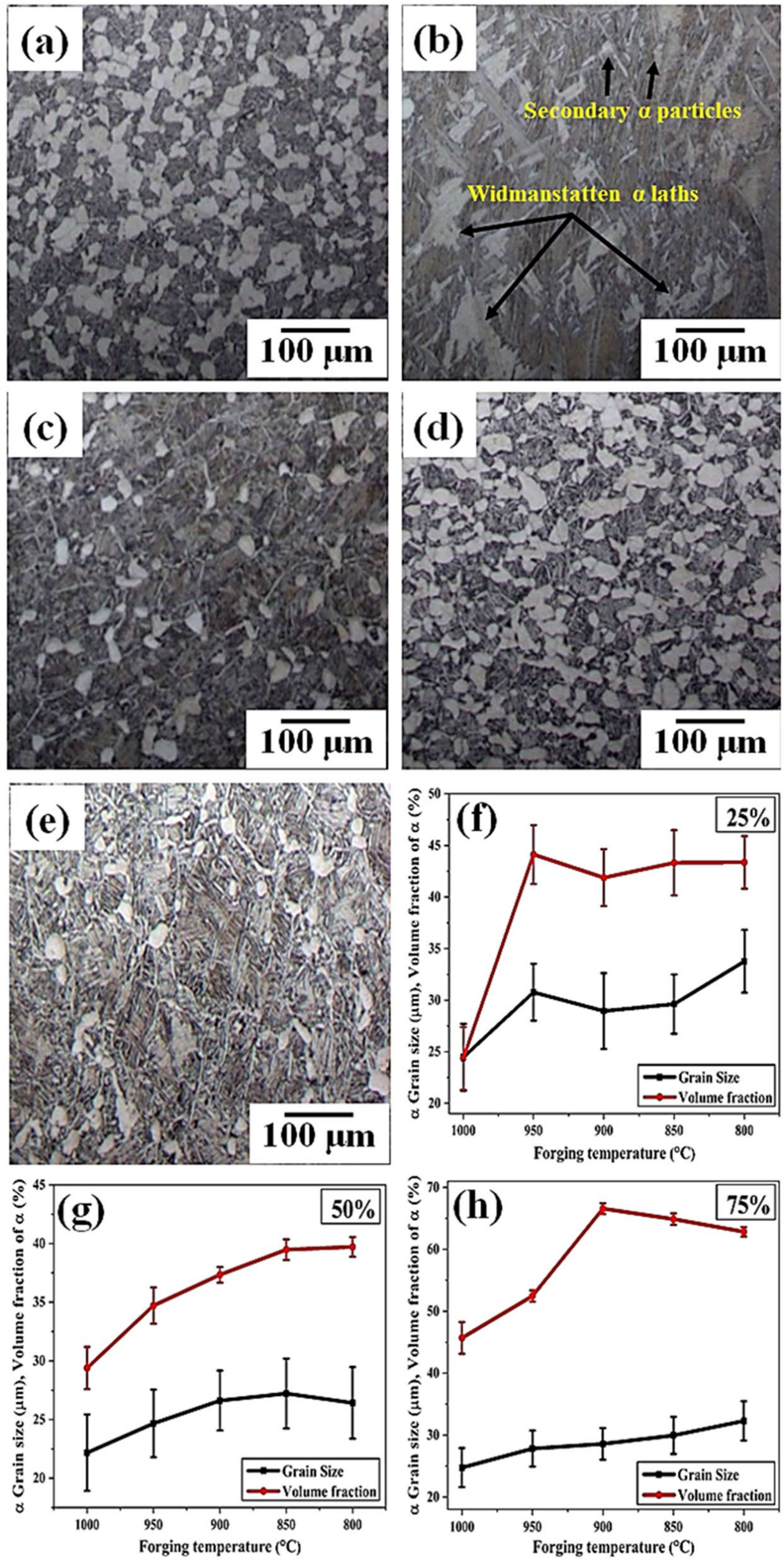

Fig. 3 OM images of Ti6Al4V forgings subjected to different % reductions followed by MA heat treatment- **a** 25% reduction at 850 °C, **b** 25% reduction at 1000 °C, **c** 50% reduction at 1000 °C, **d** 75% reduction at 800 °C and **e** 75% reduction at 1000 °C, Variation in grain size and V_f of α in MA heat-treated samples **f** 25% reduction, **g** 50% reduction, **h** 75% reduction at different prior forging temperatures

The samples forged above T_β (Fig. 3b, c) and mill annealed exhibited coarser α grain size of ~ 28 ± 2 µm, as compared to that of heat-treated sample as shown in Fig. 2c in which α grain size is ~ 15 µm. The microstructure of samples forged below T_β to 50% reduction and mill annealed (Fig. 3c) consisted of primary α as well as fine secondary

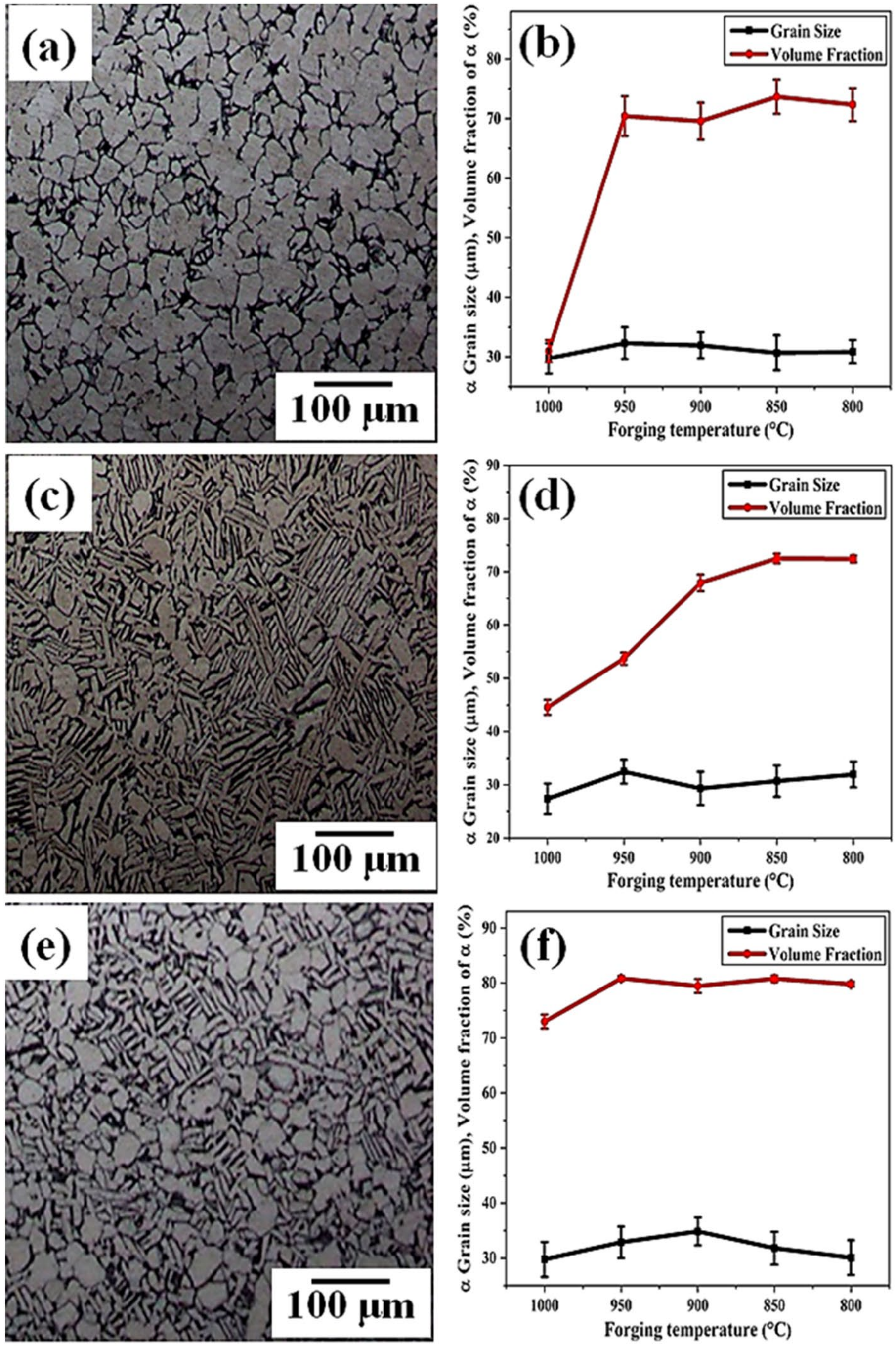

Fig. 4 OM images and corresponding variation in grain size and V_f of α with % reduction at different temperatures followed by RA heat treatment - **a** microstructure representing below T_β forging (at 950 °C) to 25% reduction and **b** variation in α grain size and V_f of α with 25% reduction, **c** representing sample forged at 1000 °C to 50% reduction and **d** variation in α grain size and V_f of α with 50% reduction, **e** representing sample forged at 1000 °C to 75% reduction and **f** variation in α grain size and V_f of α with 75% reduction

α phase in β matrix. The primary α phase was having grain size of 28 ± 2 µm and V_f of 40 ± 3% with respect to different forging temperatures. However, above T_β, the microstructure consists of Widmanstätten laths of α in a β matrix with nearly globular morphology (Fig. 3c). The corresponding V_f of equiaxed α is ~ 18 ± 2% due to finishing temperature below T_β.

With increased % reduction, a change in morphology of α can be clearly seen from as-heat treated as well as with 25% reduction sample at the same temperature. This can be attributed to adequate deformation energy available for the globularization of α phase. In 50% deformed samples, with decrease in deformation temperature, the V_f of equiaxed α was found to be marginally increasing up to 850 °C. This could be due to the combined effect of moderate reduction (50%) and forging temperature. Above T_β the Widmanstätten structure of α phase was present in β matrix where the V_f of α and grain size of α was slightly lower as compared to that of samples deformed below T_β.

The samples subjected to 75% reduction below T_β followed by mill annealing exhibited primary α grain size of 38 ± 2 µm and V_f of α phase was $62 \pm 3\%$ at various forging temperatures up to 900 °C. From forging temperature of 900 °C onwards, the V_f of α phase decreases sharply, indicating large deformation might be helping in early dissolution of α phase. Similar findings have been reported during tensile deformation of another $\alpha+\beta$ titanium alloy (Anil Kumar et al. 2019). Forging above T_β followed by mill annealing resulted in Widmanstätten lath morphology along with globular α in transformed β matrix (Fig. 3e) with a V_f of α increasing up to ~ 24%. This confirms the increasing trend of recrystallized α (secondary) with increase in amount of % reduction and finish temperature below T_β, although the deformation start temperature is above T_β. With increase in forging temperature the V_f of α phase and α grain size are found to be decreasing with minor variations (Fig. 3f–h). Minor changes in α grain size and V_f of α have been observed in as-heat treated samples also (section "Effect of heat treatment"). However, morphology of α is found to be more irregular in as-forged + mill annealed condition as compared to as-heat treated samples. The samples forged above T_β exhibited α phase colonies with acicular morphology (Fig. 3e). This is distinctly different as compared to as-heat treated sampedles where acicular α is found to be present in isolated pockets with Widmanstätten structure (Fig. 2c).

With an increase in amount of reduction, V_f of α is also found to be increasing especially from 50 to 75% reduction. This clearly indicates role of deformation in modifying the microstructure at the similar temperature due to availability of energy through deformation. Increase in V_f of equiaxed α with higher amount of reduction (75%) is observed. This is possible in higher % reduction samples due to the large deformation strain imparted to it. This also indicates that large deformation (% reduction) can lower the recrystallization temperature of alloy, which may help in recrystallization of α during forging itself (Gupta et al. 2016). The mechanism of globularization or recrystallization of α phase during deformation is also elaborated in literature on a similar titanium alloy (Anil Kumar et al. 2019).

Effect of Combination of Forging and Recrystallization Annealing Heat Treatment

In recrystallization-annealed (RA) condition (Fig. 4), the microstructure is found to be distinctly different compared to the AF + MA samples (Fig. 3). The forged microstructure transformed to microstructure consisting of recrystallized α in transformed β matrix. With 25% reduction below T_β and RA heat treatment, the grain size of α was 30 ± 2 µm in all the forged + RA conditions with respect to forging temperatures (Figs. 4a, b). The V_f of equiaxed α was almost same with respect to forging temperatures plus RA (70 ± 3). However, for the samples forged above T_β and RA heat treatment, the V_f of recrystallized equiaxed α phase was ~ 30%. Widmanstätten microstructure seen in AF condition is found to be completely modified with fine lamellar α plus basket weave microstructure along with presence of globular α.

For 50% reduction below the T_β and RA heat treatment, grain size of equiaxed α phase was almost same, i.e. 30 ± 2 µm in all the conditions with respect to forging temperatures (Fig. 4c, d). The V_f of equiaxed recrystallized α phase was (70%) also almost same in 900–800 °C forging temperatures. At 950 °C, the V_f of recrystallized equiaxed α phase reduced to ~ 58%. Above T_β, the V_f of recrystallized α phase was ~ 42% and α phase precipitation is observed in the form of short elongated α in transformed β matrix. The reduction in V_f of recrystallized α at 950 °C and above could be due to availability of stored energy in the samples subjected to large deformation (reduction %) when approaching T_β. This indicates samples deformed at relatively lower temperature result in large amount of recrystallized grains.

75% reduction below the $T_{\beta\text{-}}$ followed by RA heat-treatment resulted in similar grain size of α (30 ± 3 µm) irrespective of forging start temperatures (Fig. 4e, f). The V_f of equiaxed α phase was also found almost the same in all the conditions with respect to temperatures ($75 \pm 3\%$). Samples forged above T_β showed reduction in V_f of recrystallized α. It is due to similar reasons as mentioned for 50% reduction sample. However, the extent of reduction in V_f of recrystallized α in 75% reduction samples is slightly lower as compared to 50% reduction sample. A very unique observation is noted here in RA treated samples where V_f of recrystallized α is ~ 70–75 with 25–75% reduction, indicating important role of RA treatment.

Simplifying further, α grain size and its V_f estimation obtained through optical microscopic studies are summarized into two categories on the basis of forging temperature with respect to T_β and is presented in Table 2. It can be observed that the α grain size exhibited minor variation with change in % deformation or post deformation annealing heat treatments. However, V_f of α, which is a combination of refined primary α and recrystallized α has significant change with MA/ RA treatment. Large deformation (75%) followed by MA results in higher V_f of α, which is achievable with 25% deformation in RA treated samples (Luo and Li 2010). But further change in V_f in RA treated samples is not seen significantly with increase in % reduction. This indicates higher V_f is achievable with low to moderate deformation (25–50% reduction below T_β) followed by RA. From the results of MA and RA treated samples, higher V_f of recrystallized α and marginal change in size of α (Figs. 3 and 4) for forging below T_β can be helping to obtain uniform mechanical properties in 75% reduction + MA treated or 25–75% reduction + RA treated samples. The findings are similar to

Table 2 Estimation of α grain size and its volume fraction through optical microscopy

Conditions	Below T_β forged + heat treated		Above T_β forged + heat treated	
	α grain size (μm)	V_f (% α)	α grain size (μm)	V_f (% α)
As Heat treated	25–30	40–50	15–20	< 5
25% reduction + MA	27–33	34–42	22–28	22–28
50% reduction + MA	23–27	35–40	18–25	28–32
75% reduction + MA	33–37	55–65	22–28	42–48
25% reduction + RA	28–32	67–73	28–32	30–32
50% reduction + RA	28–32	68–70	25–30	41–42
75% reduction + RA	27–33	72–78	28–32	72–75

that reported in closed die forgings reported earlier (Gupta et al. 2016).

For the samples forged and annealed above T_β, similar increasing trend in V_f of primary α is seen for MA/ RA treated samples from 25 to 75% reduction. The change in slope of V_f of primary α (Figs. 3 and 4) with % reduction is seen where V_f increases with increasing % reduction imparted during forging. In fact, this change is noticed even at 950 °C (Fig. 3) for 75% reduction sample and MA treated. This can be attributed to larger reduction resulting in higher amount of fine recrystallized α in subsequent cooling from forging temperature assisted by MA/ RA. A significant change in V_f of primary α with % reduction is more pronounced with RA treatment due to added recrystallization process.

Microstructural Analysis Through EBSD

Selected representative samples of different conditions were analyzed using EBSD. Image quality (IQ) maps and Inverse Pole Figure (IPF) maps along with grain size charts are presented in Figs. 5 and 6. Distinct differences can be clearly seen between the AF + MA and AF + RA samples (which were prior forged at different temperatures). Samples forged at two extreme ends of temperature range and one intermediate temperature with maximum amount of deformation were analyzed. Comparing Fig. 5a1, b1, c1 with Figs. 5a2, b2, c2 reveals that samples deformed above T_β showed limited amount of α recrystallization. Close observation of AF + MA samples shows that they consist of relatively lower fraction of recrystallized grains and distribution of grains is found to be non-uniform as compared to AF + RA samples. It indicates that recrystallized fine grains of α observed in Fig. 5a1, b1, c1 could be the result of large deformation and subsequent MA, which could have contributed to some recrystallization. However, in case of a2, b2, c2 samples, temperature drop during forging, post deformation recrystallization annealing contributes a large fraction of recrystallized grains with relatively uniform distribution of α grains. Though the deformation temperature has been just above T_β, the temperature drop occurring during deformation, post deformation cooling and subsequent annealing have certainly contributed to microstructure evolution and hence the resultant microstructure.

Further, when the forging temperature is below the T_β (Fig. 5a3, b3, c3) along with post deformation RA, almost complete recrystallized grains can be observed with higher extent of uniform distribution of grains. It also indicates that a lower temperature deformation provides adequate energy for static recrystallization. Further lowering the deformation temperature shows presence of very fine grains in AF + MA condition (a4, b4, c4) as compared to higher temperature deformed + MA samples (a1, b1, c1). Similar observations were noted in optical microscopy as well. Distribution of α grains is found to be relatively non uniform in AF + MA samples. It is due to large deformation at lower temperature resulting in large amount of strain, but primary α grains are still not converted to fine grains indicating inadequacy of driving force for static recrystallization. Mill annealing normally results in reduction in residual stresses but no significant changes in the microstructure.

Further when the same sample is subjected to RA, it fully converts to recrystallized α grains (Fig. 5a5, b5, c5). But certainly, uniformity in grain size is not as observed in deformed samples at intermediate temperature (Fig. 5a3, b3, c3). It indicates that though the fraction of smaller grains may be high for lower temperature deformed + RA samples, the uniformity in grain size can be obtained only at intermediate deformation temperature.

When recrystallization occurs, the new grains are smaller in size compared to the original ones and are also strain-free. To confirm and quantify these recrystallized grains from EBSD data, two parameters are used, viz. grain size (GS) and grain orientation spread (GOS). The criteria are: GS being greater than 3 μm (since there will be no impetus for recrystallization in very small grains, typically 1 μm or less in size) and GOS less than or equal to 0.75°. Thus, grains with size > 3 μm and GOS ≤ 0.75° are treated as recrystallized (Raveendra et al. 2008). GS maps with grain of size greater than 3 μm, and GOS less than or equal to 0.75° represent the recrystallized grains and are shown in Fig. 6. Typically, if the value of GOS is more, it indicates that there is

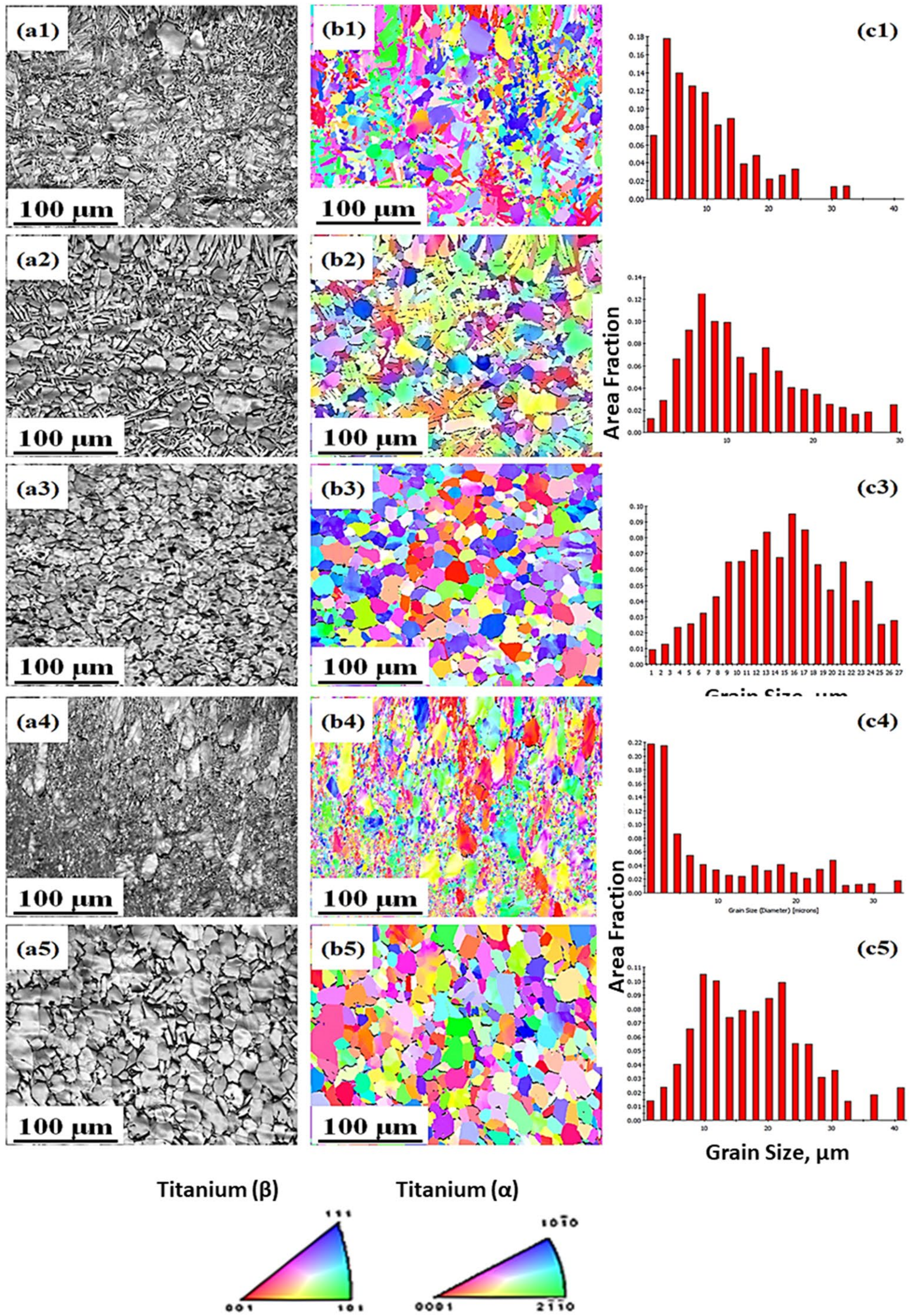

Fig. 5 EBSD maps a1-a5: IQ maps, **b1**–**b5**: IPF maps, **c1**–**c5**: Grain size area fraction plots, (**a1**, **b1**, **c1**: A7M, **a2**, **b2**, **c2**: A7R, **a3**, **b3**, **c3**:C7R, **a4**, **b4**, **c4**: E7M, **a5**, **b5**, **c5**: E7R. The EBSD maps in these figures were scanned with a step size of 0.3 µm

strain within the grain, and hence may not be a recrystallized grain. It can be seen clearly that samples C7R and E7R have a higher fraction of recrystallized grains.

Further analysis was conducted with smaller step size of 0.05 µm on specimens having maximum reduction (75%), i.e. forged at higher temperature (above T_{β}) and at lower temperature (800 °C, below T_{β}) (Fig. 7). Both the samples were selected in mill-annealed condition to analyze the extent of recrystallization. It has been clearly observed that very fine recrystallized grain nucleated in the sample forged at

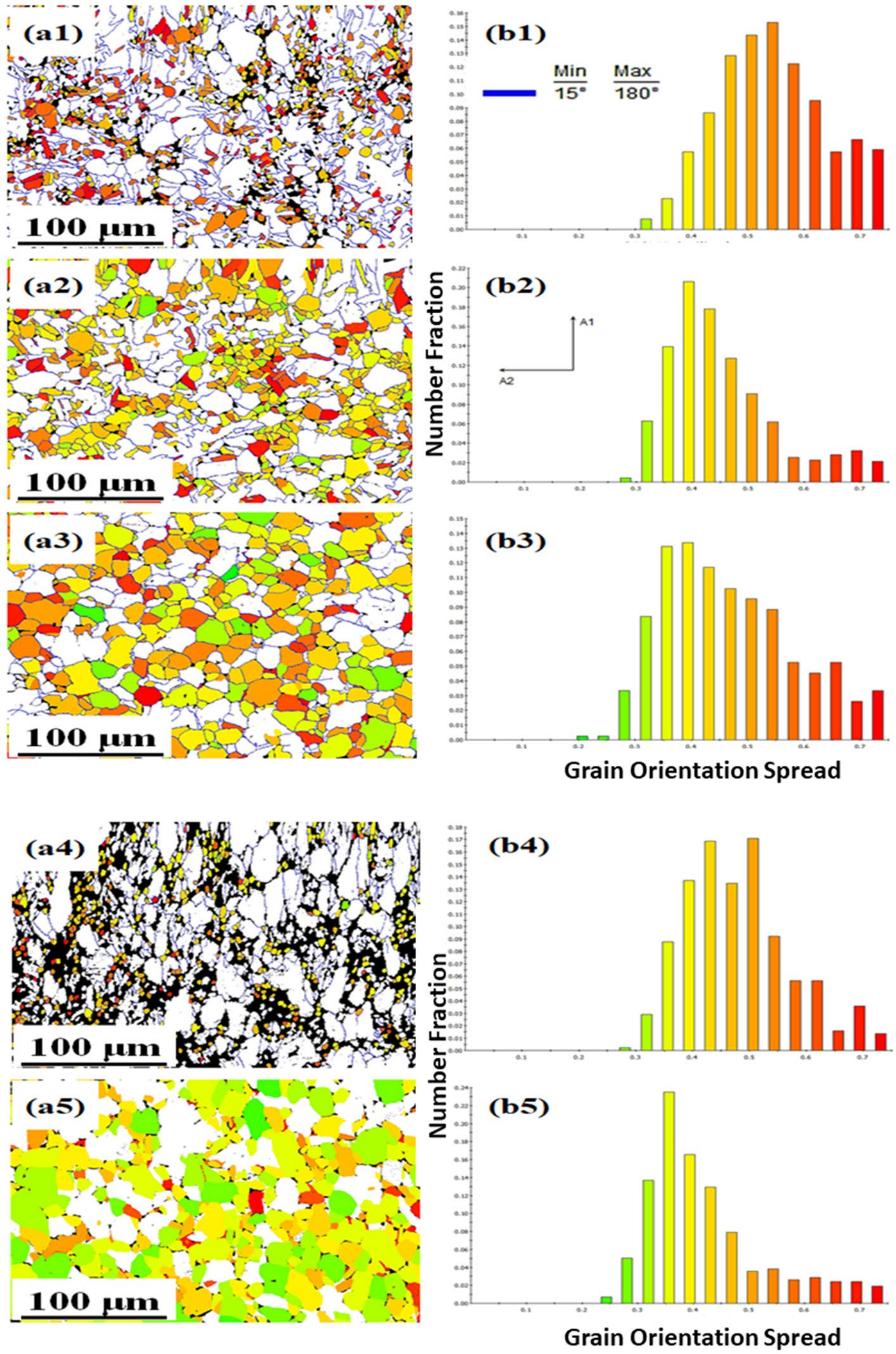

Fig. 6 GS maps (**a1**–**a5**) and GOS charts ≤ 0–0.75° (**b1**–**b5**) showing recrystallized grains (with size greater than 3 µm), (**a1**, **b1**: A7M, **a2**, **b2**: A7R, **a3**, **b3**:C7R, **a4**, **b4**: E7M, **a5**, **b5**: E7R), scanned with 0.3 µm step size (in **b1**–**b5**, the colored regions are recrystallized grains, where colors refer to the grain orientation spread, and not the crystallographic orientation)

lower temperature (E7M) along the grain boundaries of large primary α grains. The same is not observed in the sample forged at higher temperature and mill annealed (A7M). This confirms that lower temperature reduction provides sufficient stored strain energy in the material, which helps in generation of recrystallized grains during subsequent mill annealing. Also, since amount of deformation is high, lowering of actual recrystallization temperature is possible, and the same is seen as initiation of recrystallization and resulting in partially recrystallized grains. Optical microscopy also has shown presence of equiaxed recrystallized grains in sample forged at lower temperature.

A grain size analysis is also carried out through EBSD and is presented in Figs. 5, 6, 7. Summary of the grain size estimate for major area fraction obtained through EBSD is presented in Table 3. It clearly shows that recrystallization-annealed samples have relatively larger size of α grains, as compared to mill annealed samples. This is due to availability of higher driving force in the form of relatively higher temperature in recrystallization annealing. In EBSD, lower

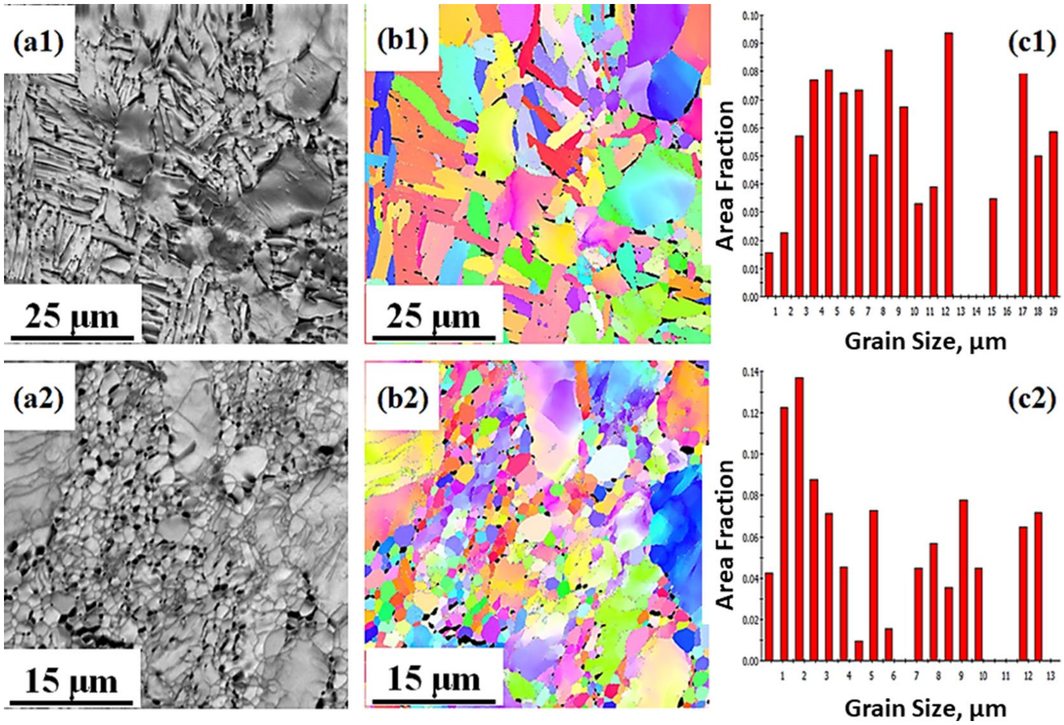

Fig. 7 EBSD maps **a1**, **a2**: IQ maps, **b1**, **b2**: IPF maps, **c1**, **c2**: Grain size area fraction plots (**a1**, **b1**, **c1**: A7M, **a2**, **b2**, **c2**: E7M, with 0.05 μm step size)

Table 3 α Grain size estimate obtained through EBSD from Fig. 6

Sample Id No.	α grain size, μm
A7M	< 15
A7R	5–15
C7R	10–20
E7M	< 10
E7R	10–20

size of α grains are revealed as compared to observation made through optical microscopy due to higher resolution images in EBSD. Also, it is analyzed in relatively very small area in EBSD. However, both optical microscopy and EBSD results are found to be complementing each other.

Mechanical Property Evaluation

Tensile and Impact Strength

Tensile testing of as-heat treated samples as well as forged + annealed samples was carried out. The nature of stress–strain curves for as-heat treated samples and forged plus annealed samples at respective temperatures is found to be similar. Typical examples of samples tested in as-heat treated, forged + annealed conditions are presented in Fig. 8.

Mechanical properties of different heat-treated samples are given in Table 4. The 0.2% offset yield stress (YS) of higher temperature forged + MA sample shows marginal increase as compared to heat-treated samples at respective temperatures, possibly due to α refinement in microstructure during forging. However, the same is not seen in UTS. At the same time, impact strength is found to be consistently low for the samples forged at all the temperatures as compared to the as-heat treated samples. This also indicates that microstructural refinement of the α lamellae structure, which normally results in higher fracture toughness and impact strength gets fragmented during forging and the microstructure is refined. Further, V_f of α also plays an important role. In as-heat treated condition, transformed β phase in the matrix shall be higher, which contributes to higher impact strength.

In similar lines, 50% reduction + MA samples exhibited higher 0.2% offset yield stress in all the samples except those forged at 1000 °C. This can be attributed to occurrence of large amount of microstructure refinement of α. Unlike 25% reduction + MA samples, UTS is found to be higher than that of heat-treated as well as 25% reduction + MA samples. This indicates that higher amount of % reduction contributes towards generation of more lattice defects and α phase refinement. It is also found that impact strength is in similar lines of 25% reduction + MA samples, indicating microstructure refinement of α is affecting impact properties as explained earlier. 1000 °C forged + MA sample exhibited no significant change as compared to heat-treated samples.

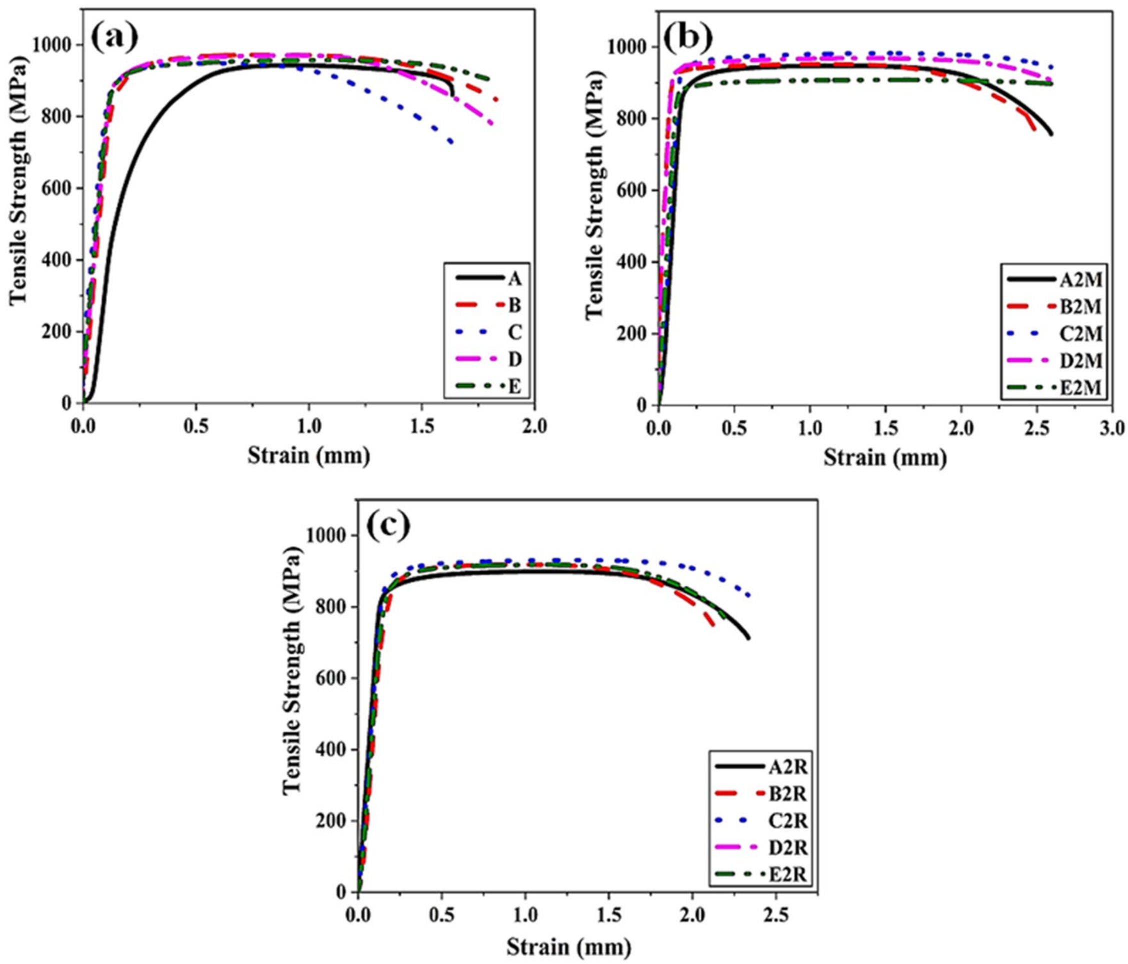

Fig. 8 Representative plots of engineering stress–strain curves of Ti6Al4V in **a** As received + Heat Treated at different temperatures, **b** 25% reduction + MA heat-treated condition, **c** 25% reduction + RA heat treatment condition. Note: All testing has been done at room temperature

Minor reduction in 0.2% offset yield stress is observed as compared to 25% reduction + MA samples. It indicates that two or more opposite factors are working at higher temperatures. It may be possible that benefit of higher amount of reduction through microstructure refinement of α is balanced by high temperature forging especially above T_{β}.

In 75% reduction + MA samples, the trend is similar to 50% reduction + MA samples. Marginally higher 0.2% offset YS in 75% reduction + MA sample are in expected lines due to presence of higher amount fine grains. However, marginal reduction in 0.2% offset YS and UTS is seen for the samples forged at lower temperature (E7M). This can be attributed to large extent of recrystallization in subsequent annealing, as observed through optical microscopy and EBSD. Also, this has been clearly indicated by the V_f of α. Impact strength in 75% deformed + MA condition is seen to be marginally lower than other three conditions indicating refinement of α microstructure resulting in mainly equiaxed morphology of microstructure or minimum amount of lamellar structure. However, low-temperature deformation (E7M) resulted in higher impact strength indicating role of recrystallization.

In RA condition, as the alloy is subjected to recrystallization annealing at 930 °C, the previous history of deformation up to RA temperature modifies significantly in recrystallization phenomenon changing the microstructure to fine recrystallized microstructure (Figs. 5, 7, 8). The mechanical properties are thereby governed by such microstructural changes. With 25–75% reduction and RA, 0.2% offset YS of alloy exhibits marginal change in higher temperature forged samples (1000 °C). However, in case of lower temperature forged samples 0.2% offset YS were similar to that obtained in as-heat treated samples at respective temperatures but it has reduced strength as compared to forged + MA condition at respective temperatures with same amount of % reduction, respectively. Minor change in strength for high temperature worked structure (1000 °C) and RA treated can be attributed to limited α refinement in microstructure. However, impact strength is found to be marginally higher as compared to

Table 4 Room temperature mechanical properties of Ti6Al4V in different heat-treated conditions without and with different prior forging reductions

Sl. No	Id	Forging start Temp (°C)	0.2% Offset YS (MPa)	UTS (MPa)	% El (GL = 4d)	Impact strength (Kg-m/cm^2)
1	A	1000	861	961	10	3.1
2	B	950	886	968	17	3.1
3	C	900	861	945	18	3.3
4	D	850	890	950	19	2.6
5	E	800	886	960	18	2.4
6	A2M	1000	882	951	20	2.6
7	B2M	950	878	945	17	2.4
8	C2M	900	900	961	21	2.1
9	D2M	850	910	969	21	2.3
10	E2M	800	874	929	22	2.2
11	A2R	1000	858	899	19	2.8
12	B2R	950	871	919	20	2.9
13	C2R	900	878	931	20	2.8
14	D2R	850	880	932	19.5	2.9
15	E2R	800	887	919	20	2.7
16	A5M	1000	867	973	18	2.5
17	B5M	950	921	972	16	2.2
18	C5M	900	951	986	16	2.1
19	D5M	850	965	1000	14.5	2.1
20	E5M	800	978	1005	18	2.2
21	A5R	1000	854	906	20	2.3
22	B5R	950	886	937	19	3.1
23	C5R	900	879	927	22	2.9
24	D5R	850	870	917	23.5	3.2
25	E5R	800	869	915	23	2.5
26	A7M	1000	931	997	14.5	2.1
27	B7M	950	958	1012	15	2.0
28	C7M	900	955	1002	14	1.9
29	D7M	850	967	1012	15	2.2
30	E7M	800	958	990	17	2.8
31	A7R	1000	879	963	19.5	2.6
32	B7R	950	856	926	18	2.7
33	C7R	900	880	940	15	2.5
34	D7R	850	865	937	16	2.8
35	E7R	800	860	934	16	2.8

deformed + MA samples, but it is marginally lower than that of as-heat treated condition sample. This indicates higher recrystallization may be helping to improve impact strength.

Minor variation in trend is noted in the mechanical properties with respect to % reduction and deformation temperature. But it is certainly clear that, RA is playing a significant role in bringing uniformity in mechanical properties as observed in the V_f of α, that is almost similar in forged samples (25–75%) after RA treatment. Marginal increase in impact strength for deformed and RA heat-treated samples indicate more recrystallization though it reduces strength, a marginal increase in impact strength is observed. It is due to increased grain boundary area resultant fine recrystallized grains and generation of large amount of low angle boundary (Balasubramanian et al. 2008; Wen et al. 2019).

Three important factors are found to be playing a significant role in deciding the mechanical properties, viz. presence of acicular α from near T_β exposure/deformation, refinement of primary α grains during deformation and extent of recrystallization (generation of new recrystallized α grains). First factor plays a predominant role in high-temperature heat treatment/ deformation. The second factor plays a predominant role at temperature below T_β and higher amount of deformation with MA resulting in refined primary α. The third factor is predominant in large deformation combined with MA or RA resulting in mainly recrystallized α. Accordingly, variation in mechanical properties is observed. Moderate cooling from higher temperature will result in formation of large amount of acicular α whereas large deformation at lower temperature provides opportunity of grain refinement/recrystallization. Analyzing the results in this study, it can be inferred that large amount of deformation, which results in refinement of primary α grains provides improvement in tensile strength with marginal reduction in impact strength. Further higher amount of deformation, which is associated with recrystallization, showed marginal reduction in tensile strength and minor improvement in impact strength.

% Elongation to Failure

% Elongation to failure is found to be consistent in heat-treated conditions below the T_β (17–18%). The sample heat treated above T_β exhibited lower % elongation due to the fully transformed β microstructure. However, the same is not seen in 25% reduction + annealed sample, where elongation is consistently higher (20–21%) with marginal improvement compared to the as-heat treated samples indicating effect of α microstructure refinement. However, at 50% as well as at 75% reduction + MA conditions, % elongation exhibited a marginal drop (14.5–16%). Elongation is found to be consistently high in forged + RA samples. This could be due to extensive deformation and its effect on extent of recrystallization during RA according to forging temperature.

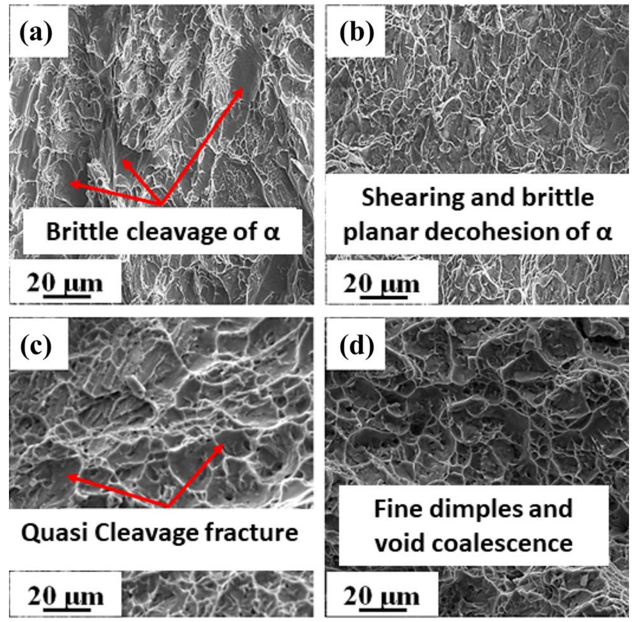

Fig. 9 Representative fractographs of Ti6Al4V impact samples heat treated at **a** 1000 °C and **b** 800 °C; fractographs of Ti6Al4V tensile samples heat treated at **c** 1000 °C and **d** 800 °C. Note: All testing has been done at room temperature

Fractography

Fractography of impact-tested and tensile-tested samples was carried out through SEM and the analysis is presented in subsequent sections.

As-Heat Treated Condition

The presence of large grains in samples heat treated above T_β resulted in Widmanstätten structure with α plates. In impact testing, it helped to absorb large amount of energy thereby resulting in higher impact strength. The same is seen in fractography (Fig. 9a) showing larger fragmentation of α plates as compared to other sample heat-treated below T_β (Fig. 9b), where impact strength is marginally low.

However, tensile elongation is found to be lower in samples heat treated above T_β as compared to the samples heat treated below the T_β. Similarly, quasi-cleavage features are observed in fractographs of impact specimen as shown in Fig. 9c which indicates the microstructure consists of significant fraction of transformed β. The sample heat treated at 800 °C as shown in Fig. 9d, exhibited substantially higher amount of dimples as compared to Fig. 9c. This indicates importance of nearly equiaxed primary α in transformed β microstructure resultant of heat treatment below the T_β to result in ductile failure in tensile or impact modes of deformation.

Forged + Heat Treated Condition

The effect of 25% reduction during forging on tensile and impact properties is found to be not significant. The impact strength is higher for the sample forged above T_β and subjected to MA heat treatment as compared to the sample forged below the T_β and subjected to MA heat treatment. In fractography, significant differences are not observed among different conditions. Fine dimples could be observed in most of the samples subjected to tensile testing as shown in Fig. 10a indicating presence of microstructure resultant of higher temperature deformation, which assisted in formation of acicular α in Widmanstätten structure. This can result in higher impact energy absorption through crack propagation as shown in Fig. 10b.

Hot forging followed by RA heat treatment modified the microstructure and corresponding mechanical properties significantly. Large reduction at lower temperature has resulted in marginally high impact strength as compared to higher temperature forged sample (above T_β). Very fine dimples along with flat cleavage type, i.e. mixed mode of fracture could be observed in sample forged at above T_β + RA heat treatment followed by tensile testing

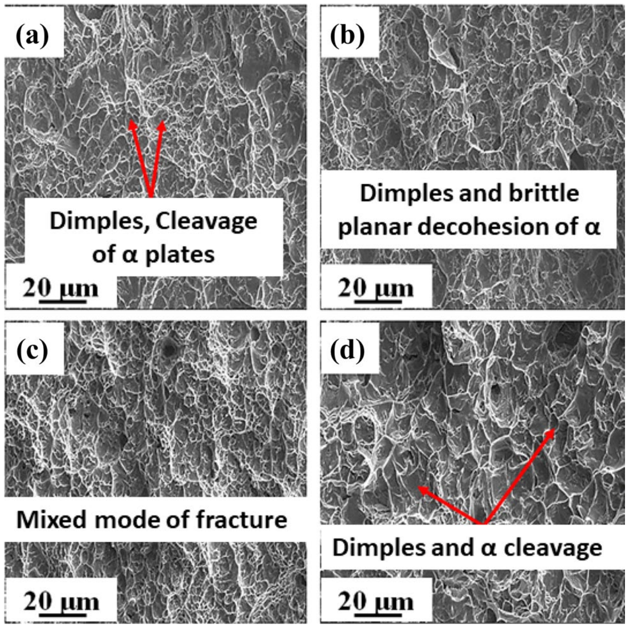

Fig. 10 Representative fractographs of Ti6Al4V samples subjected to 25% reduction at 1000 °C + MA heat treatment- **a** tensile-tested and **b** impact-tested specimens, 25% reduction at 1000 °C + RA heat treatment- **c** tensile-tested and **d** impact-tested specimens. Note: All testing has been done at room temperature

indicating highly refined Widmanstätten microstructure due to large % reduction (Fig. 10c). Sample subjected to impact testing showed large amount of deformation, i.e. deeper dimples (Fig. 10d) compared to Fig. 10b resulting in marginally higher impact strength through more energy absorption. So it can be concluded that higher grain boundary area either through lamellar structure or through large volume of very fine recrystallized α grains shall be helping in improving the impact strength.

For samples subjected to 50% reduction, significant effect of RA was observed with more consistent elongation in tensile loading. In case of impact testing, though the sample forged above T_β may contain some remnants of transformed β microstructure, due to large deformation and RA heat treatment, significant effect of higher temperature deformation is not dominant. Similar is the case for tensile testing. In all these cases, the mechanical properties are more consistent and corresponding fractographs were having mostly similar features.

At large reduction of 75%, the impact strength of samples forged above T_β are similar to the samples forged below T_β. The fracture surfaces are mostly similar with presence of fine dimples. Here, the benefit of large deformation and RA is highly effective in bringing uniformity in microstructure towards equiaxed morphology and correspondingly the fracture surface.

Conclusions

The titanium alloy Ti6Al4V was hot forged at different temperatures and with different % reduction followed by mill annealing (MA) and recrystallization annealing (RA) heat treatments. The following conclusions are drawn from the present study:

1. Heat treatment/ forging above T_β led to significant presence of Widmanstätten structure, which lowered the strength, but led to marginal improvement in the impact strength.
2. Samples forged below T_β showed improvement in strength in mill-annealed (MA) condition due to α grain refinement during deformation and further partial recrystallization during heat treatment.
3. Forging with 25–50% reduction at intermediate temperatures (850–900 °C) + MA heat treatment resulted in higher strength as compared to either lower temperature deformation or deformation above T_β. However, with further increase in % reduction to 75%, improvement in strength is not seen due to large amount of recrystallization of α phase due to combination of reduction and subsequent MA heat treatment.
4. The α phase refinement as well as V_f of primary α is found to be lower in samples deformed at high temperatures ~ T_β., whereas in samples forged at lower temperature, the refinement of α is observed and its V_f is high.
5. Impact strength is found to be moderate to low with increased % reduction followed by MA heat treatment. However minor improvement is observed in samples subjected to large deformation + MA heat treatment, implying that very fine recrystallized α contributes to the improvement in impact strength. Impact strength is also found to be relatively higher in RA condition further indicating completely recrystallized α grains improve the impact strength.
6. Similar trend in strength with lesser scatter is observed in forged + RA condition at different amounts of deformation. Marginally lower strength in RA condition is attributed to presence of large extent of recrystallized α.
7. Fraction of smaller grains is higher for lower temperature deformed + RA heat-treated samples, but the uniformity in α grain size is obtained at intermediate deformation temperature (850–900 °C).
8. Large deformation results in refined primary α grains and results in improvement in tensile strength with marginal reduction in impact strength. Deformation associated with α recrystallization resulted in minor reduction in tensile strength and improvement in

impact strength obtained through low-temperature and large deformation reduction + RA or MA heat treatment.

9. % Elongation is found to be varying (14–18%) in MA conditions and further higher elongation was observed in samples subjected to RA heat treatment.
10. Samples forged below T_β followed by heat treatment (MA/ RA) exhibited predominantly ductile features, whereas samples forged above T_β exhibited cleavage-type fracture features.

Acknowledgements Authors are also grateful to MPD, MCD, VSSC for the experimental work support. Authors express their gratitude to GM, MMA, DD, MME for guidance during this work and Director, VSSC for granting permission to publish this work.

Funding This work did not receive any funding from any external funding agency.

Availability of data and material The data are a part of continuing research and hence cannot be shared at this point of time.

Code availability There is no code used in this activity.

Declarations

Conflict of interest The authors do not have any conflict/ competing interests with anyone/ any groups.

References

Aerospace Material Specification (2017) Ultrasonic inspection titanium and titanium alloy bar, billet and plate AMS2631E. SAE International, Warrendale, pp 1–17

Anil Kumar V, Gupta RK, Chakravadhanula VSK, Gourav Rao A, Prasad MJNV, Murty SVSN (2019) Effect of test temperature on tensile behavior of Ti-5Al-5V-2Mo-1Cr-1Fe (α+β) titanium alloy with initial microstructures in hot forged and heat treated conditions. Met Mater Trans A 50–6:2702–2719. https://doi.org/10.1007/s11661-019-05207-y

Balasubramanian M, Jayabalan V, Balasubramanian V (2008) Effect of microstructure on impact toughness of pulsed current GTA welded α-β titanium alloy. Mater Lett 62:1102–1106. https://doi.org/10.1016/j.matlet.2007.07.065

Chao Q, Cizek P, Wang J, Hodgson PD, Beladi H (2016) Enhanced mechanical response of an ultrafine grained Ti-6Al-4V alloy produced through warm symmetric and asymmetric rolling. Mater Sci Eng A 650:404–413. https://doi.org/10.1016/j.msea.2015.10.061

Chong Y, Bhattacharjee T, Yi J, Zhao S, Tsuji N (2019) Achieving bi-lamellar microstructure with both high tensile strength and large ductility in Ti–6Al–4V alloy by novel thermomechanical processing. Materialia 8:100479. https://doi.org/10.1016/j.mtla.2019.100479

Ding R, Guo ZX (2004) Microstructural evolution of a Ti-6Al-4V alloy during β-phase processing: experimental and simulative investigations. Mater Sci Eng A 365:172–179. https://doi.org/10.1016/j.msea.2003.09.024

Ding R, Guo ZX, Wilson A (2002) Microstructural evolution of a Ti-6Al-4V alloy during thermomechanical processing. Mater Sci Eng A 327:233–245. https://doi.org/10.1016/S0921-5093(01)01531-3

Flower HM (1990) Microstructural development in relation to hot working of titanium alloys. Mater Sci Technol 6:1082–1092

Gerhard W, Boyer R, Collings EW (1993) Materials properties handbook: titanium alloys. ASM International Materials Park, Novelty

Guo Z, Malinov S, Sha W (2005) Modelling beta transus temperature of titanium alloys using artificial neural network. Comput Mater Sci 32:1–12. https://doi.org/10.1016/j.commatsci.2004.05.004

Gupta RK, Arumugam M, Karthikeyan MK, Pant B, Ghosh BR (2007) Investigation of ultrasonic indications in Ti alloy (Ti6Al4V) hot formed hemisphere. Eng Fail Anal 14:1286–1293. https://doi.org/10.1016/j.engfailanal.2006.11.033

Gupta RK, Anil Kumar V, Ramkumar P (2016) Effect of variants of thermomechanical working and annealing treatment on titanium alloy Ti6Al4V closed die forgings. J Mater Eng Perform 25:2551–2562. https://doi.org/10.1007/s11665-016-2110-8

Gupta RK, Anil Kumar V, Gaur R, Singh BK (2018a) Effect of heat treatment and combination of cold rolling and heat treatment on microstructure and mechanical properties of titanium alloy Ti6Al2V2Zr1.5Mo. J Mater Eng Perform 27:4405–4422. https://doi.org/10.1007/s11665-018-3576-3

Gupta RK, Anil Kumar V, Ramkumar P, Gururaja UV (2018b) Development of large-sized titanium alloy Ti6Al4V and nickel-based superalloy inconel-718 forgings for reusable launch vehicle-technology demonstrator flight. Curr Sci 114(1):131–136. https://doi.org/10.18520/cs/v114/i01/131-136

Kim YW, Boyer RR (1991) Microstructure/property relationships in titanium aluminides and alloys. In: Proc. Symp. Fall Meet. Miner. Met. Mater. Soc., pp 7–11

Lin YC, Jiang XY, Jun Shuai C, Zhao CY, He DG, Chen MS, Chen C (2018) Effects of initial microstructures on hot tensile deformation behaviors and fracture characteristics of Ti-6Al-4V alloy. Mater Sci Eng A 711:293–302

Luo J, Li M, Yu W (2010) Microstructure evolution during high temperature deformation of Ti-6Al-4V alloy. Rare Met Mater Eng 39:1323–1328. https://doi.org/10.1016/s1875-5372(10)60114-2

Lütjering G (1998) Influence of processing on microstructure and mechanical properties of (α + β) titanium alloys. Mater Sci Eng A 243:32–45. https://doi.org/10.1016/s0921-5093(97)00778-8

Lütjering G, Albrecht J, Ivasishin OM (1994) Microstructure/property relationships of titanium alloys. TMS, Warrendale, pp 65–74

Nieh TG, Wadsworth J, Sherby OD (2005) Superplasticity in metals and ceramics. Cambridge University Press, Cambridge

Prasad K, Kumar V (2011) Isothermal and thermomechanical fatigue behaviour of Ti-6Al-4V titanium alloy. Mater Sci Eng A 528:6263–6270. https://doi.org/10.1016/j.msea.2011.04.085

Raveendra S, Mishra S, Mani Krishna KV, Weiland H, Samajdar I (2008) Patterns of recrystallization in warm- and hot-deformed AA6022. Metall. Mater Trans A Phys Metall Mater Sci 39:2760–2771. https://doi.org/10.1007/s11661-008-9620-4

Seetharaman V, Boothe L, Lombard CM (1991) Microstructure/property relationships in titanium aluminides and alloys the minerals, metals and materials society. TMS, Warrendale, p 605

Seshacharyulu T, Medeiros SC, Frazier WG, PrasadYVRK, (2000) Hot working of commercial Ti-6Al-4V with an equiaxed α-β microstructure: Materials modeling considerations. Mater Sci Eng A 284:184–194. https://doi.org/10.1016/s0921-5093(00)00741-3

Shaikh A, Kumar S, Dawari A, Kirwai S, Patil A, Singh R (2019) Effect of temperature and cooling rates on the α+β morphology of Ti-6Al-4V alloy. Proced Struct Integr 14:782–789. https://doi.org/10.1016/j.prostr.2019.07.056

Smith WF (1993) Structure and properties of engineering alloys, 2nd edn. McGraw-Hill, New York

Welsch G, Weiss I, Eylon D, Froes FH (1988) In: Lacombe R, Tricot GB (eds) Sixth World Conference on Titanium, Part III, Societe Francais de Metallurgie, Les Ulis Cedex, France, June 6–9, p 1289

Wen X, Wan M, Huang C, Tan Y, Lei M, Liang Y, Cai X (2019) Effect of microstructure on tensile properties, impact toughness and fracture toughness of TC21 alloy. Mater Des 180:107898. https://doi.org/10.1016/j.matdes.2019.107898